

Experimental studies of the coherence of microstructure-fiber supercontinuum

Xun Gu, Mark Kimmel, Aparna P. Shreenath and Rick Trebino

School of Physics, Georgia Institute of Technology, Atlanta, GA 30332-0430, USA
xun.gu@physics.gatech.edu

John M. Dudley

Laboratoire d'Optique P. M. Duffieux, Université de Franche-Comté, F-25030 Besançon, France

Stéphane Coen

Service d'Optique et Acoustique, Université Libre de Bruxelles, B-1050 Brussels, Belgium

Robert S. Windeler

OFS Fitel Laboratories, 700 Mountain Ave., Murray Hill, NJ 07974, USA

Abstract: The phase coherence of supercontinuum generation in microstructure fiber is quantified by performing a Young's type interference experiment between independently generated supercontinua from two separate fiber segments. Analysis of the resulting interferogram yields the wavelength dependence of the magnitude of the mutual degree of coherence, and a comparison of experimental results with numerical simulations suggests that the primary source of coherence degradation is the technical noise-induced fluctuations in the injected peak power.

©2003 Optical Society of America

OCIS codes: (320.0320) Ultrafast optics; (190.4370) Nonlinear optics, fibers; (999.999) Microstructure fibers; (999.999) Photonic crystal fibers

References and links

1. S. A. Diddams, D. J. Jones, J. Ye, T. Cundiff, J. L. Hall, J. K. Ranka, R. S. Windeler, R. Holzwarth, T. Udem, and T. W. Hänsch, "Direct link between microwave and optical frequencies with a 300 THz femtosecond laser comb," *Phys. Rev. Lett.* **84**, 5102-5105 (2000).
2. A. V. Husakou and J. Herrmann, "Supercontinuum generation of higher-order solitons by fission in photonic crystal fibers," *Phys. Rev. Lett.* **8720**, 203901 (2001).
3. A. L. Gaeta, "Nonlinear propagation and continuum generation in microstructured optical fibers," *Opt. Lett.* **27**, 924-926 (2002).
4. J. M. Dudley and S. Coen, "Coherence properties of supercontinuum spectra generated in photonic crystal and tapered optical fibers," *Opt. Lett.* **27**, 1180-1182 (2002).
5. X. Gu, L. Xu, M. Kimmel, E. Zeek, P. O'Shea, A. P. Shreenath, R. Trebino, and R. S. Windeler, "Frequency-resolved optical gating and single-shot spectral measurements reveal fine structure in microstructure-fiber continuum," *Opt. Lett.* **27**, 1174-1176 (2002).
6. T. M. Fortier, J. Ye, S. T. Cundiff, and R. S. Windeler, "Nonlinear phase noise generated in air-silica microstructure fiber and its effect on carrier-envelope phase," *Opt. Lett.* **27**, 445-447 (2002).
7. K. L. Corwin, N. R. Newbury, J. M. Dudley, S. Coen, S. A. Diddams, B. R. Washburn, K. Weber, and R. S. Windeler, "Fundamental amplitude noise limitations to supercontinuum spectra generated in a microstructured fiber," *Appl. Phys. B* **77**, 269-277 (2003).
8. T. M. Fortier, D. J. Jones, J. Ye, S. T. Cundiff, and R. S. Windeler, "Long-term carrier-envelope phase coherence," *Opt. Lett.* **27**, 1436-1438 (2002).
9. M. Bellini and T. W. Hänsch, "Phase-locked white-light continuum pulses: toward a universal optical frequency-comb synthesizer," *Opt. Lett.* **25**, 1049-1051 (2000).
10. P. Baum, S. Lochbrunner, J. Piel, and E. Riedle, "Phase-coherent generation of tunable visible femtosecond pulses," *Opt. Lett.* **28**, 185-187 (2003).
11. J. K. Ranka, R. S. Windeler, and A. J. Stentz, "Visible continuum generation in air-silica microstructure optical fibers with anomalous dispersion at 800 nm," *Opt. Lett.* **25**, 25-27 (2000).

12. M. Nakazawa, K. Tamura, H. Kubota, and E. Yoshida, "Coherence degradation in the process of supercontinuum generation in an optical fiber," *Opt. Fiber Technol.* **4**, 215-223 (1998).
13. J. Herrmann, U. Griebner, N. Zhavoronkov, A. Husakou, D. Nickel, J. C. Knight, W. J. Wadsworth, P. S. J. Russell, and G. Korn, "Experimental evidence for supercontinuum generation by fission of higher-order solitons in photonic fibers," *Phys. Rev. Lett.* **88**, art. no.-173901 (2002).
14. H. Kubota, K. R. Tamura, and M. Nakazawa, "Analyses of coherence-maintained ultrashort optical pulse trains and supercontinuum generation in the presence of soliton-amplified spontaneous-emission interaction," *J. Opt. Soc. Am. B* **16**, 2223-2232 (1999).
15. P. D. Drummond and J. F. Corney, "Quantum noise in optical fibers. I. Stochastic equations," *J. Opt. Soc. Am. B* **18**, 139-152 (2001).

Supercontinuum (SC) generation in microstructure fiber has now been reported under a variety of experimental conditions, and has found particularly important applications in optical frequency metrology [1]. Although SC generation is complex, several studies have now identified the dominant spectral broadening mechanisms, providing insight into the stability (or the lack thereof) of the generated SC [2-4]. Numerical simulations, in particular, have shown that SC generation can exhibit extreme sensitivity to input pulse noise, leading to both shot-to-shot intensity fluctuations which can wash out spectral fine structure and shot-to-shot phase fluctuations that degrade the SC coherence [3, 4]. These predictions were confirmed experimentally by frequency-resolved optical gating (FROG) and single-shot spectral measurements [5], and by using RF noise analysis to measure both the relative intensity noise [6, 7] and the long-term carrier-envelope phase coherence [8].

The SC coherence can also be conveniently quantified by interfering together independently generated SC in a Young's two source type experiment. This technique, first reported by Bellini and Hänsch in the context of SC generation in bulk media [9], has also recently been used to quantify the relative coherence of independently seeded optical parametric amplifiers [10]. In this paper, we report the first use of this method to characterize the coherence of microstructure fiber SC by interfering together two SC generated in different fiber segments, and in particular, we carry out a quantitative analysis of the resulting interferogram that allows the wavelength dependence of the mutual degree of coherence to be determined. A comparison with stochastic nonlinear Schrödinger equation (NLSE) simulations shows that the observed coherence degradation is consistent with fluctuations in the injected peak power significantly higher than the quantum limit. The significance of measuring the mutual coherence function is that it is the most natural measure of the phase coherence of light, and that experiments sensitive to phase stability will, in general, depend on it in some way. For SC generation, it provides an extremely useful measure of the sensitivity of the spectral broadening processes to input pulse noise, allowing the optimization of experimental design to ensure coherent SC generation.

Our experiments used a 90 MHz repetition rate KM Labs Ti:Sapphire laser generating transform-limited 60 fs pulses at 800 nm. The pulses were injected into Lucent Technologies microstructure fiber with zero-dispersion wavelength ≈ 770 nm [11]. Before using the Bellini-Hänsch technique for coherence measurements, a preliminary study of the SC phase stability was performed using a straightforward spectral interference experiment between a typical microstructure-fiber-generated SC, and a picked-off fraction of the laser pump pulses. Fig. 1 shows these results for an 18 cm fiber length and an injected pulse energy of 1 nJ. Distinct interference fringes are observed in the overlap region of the two spectra, suggesting that some coherence with the pump pulses is maintained during the SC generation process.

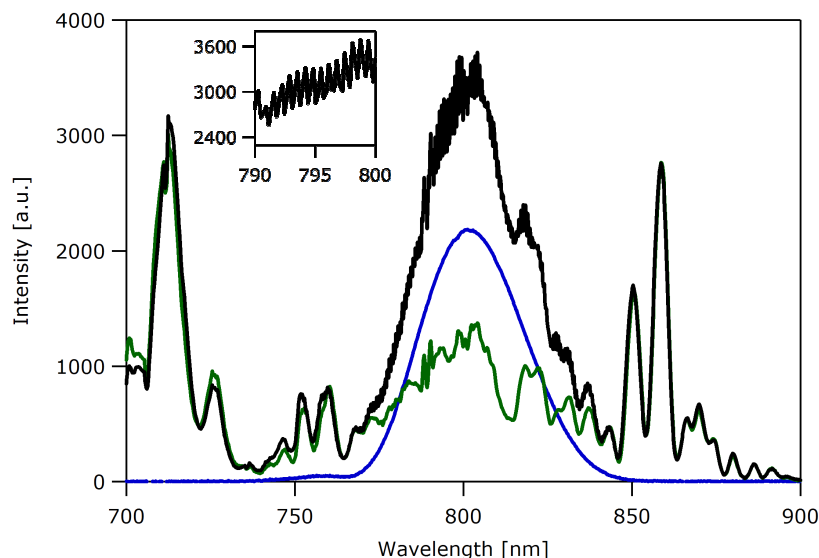


Fig. 1. Spectral interference of a generated SC with the Ti:Sapphire pump pulse. Shown in the plot are the spectra of: the microstructure-fiber SC (green line), the Ti:Sapphire output (blue line), and the interference spectrum of the two (black line). The inset shows an expanded section of the interference spectrum around 795 nm.

The presence of this residual pump-SC coherence is *a priori* surprising, as both numerical simulations of SC generation and spectral broadening in both microstructure fiber [3, 4] and standard fibers [12] have shown strong coherence degradation due to the amplification of input pulse noise. Moreover, cross-correlation FROG measurements of microstructure fiber SC generation have also shown strong shot-to-shot instabilities [5]. In this context, however, we note that the numerical studies in Refs. [3, 4, 7] have shown that the robustness of the SC generation process to input pulse noise (and hence the output SC coherence) depends strongly on the input pulse parameters, and the use of sub-100 fs pulses would be expected to preserve some degree of spectral phase coherence even in the presence of significant spectral broadening. The residual coherence measured here using 60-fs pulses is consistent with these numerical results.

As has been discussed in detail in Refs. [4, 7], the dependence of the supercontinuum coherence on the input pulse duration can be understood physically in terms of the interplay between the spectral broadening processes associated with soliton fission [13] and modulational instability or four wave mixing [14]. With pulses injected in the anomalous dispersion regime, the initial pulse is viewed as a higher-order soliton that splits into individual fundamental solitons at different center wavelengths. However, because modulational instability gain amplifies any fluctuations present on the input pulse envelope, this process is extremely sensitive to the presence of any input pulse noise. The degree of sensitivity depends on the distance scale over which soliton fission occurs: for shorter pulses where fission occurs over a shorter propagation distance, modulational instability gain (which scales as the product of peak power and length) does not play as significant a role in perturbing the pulse break-up process and thus the resulting broadband spectrum exhibits higher intensity stability and phase coherence. This can also be understood by considering that, for injected pulses with the same energy but different durations, shorter input pulses are associated with a lower soliton number so that the degree of soliton fission and hence the sensitivity to input pulse noise is lower.

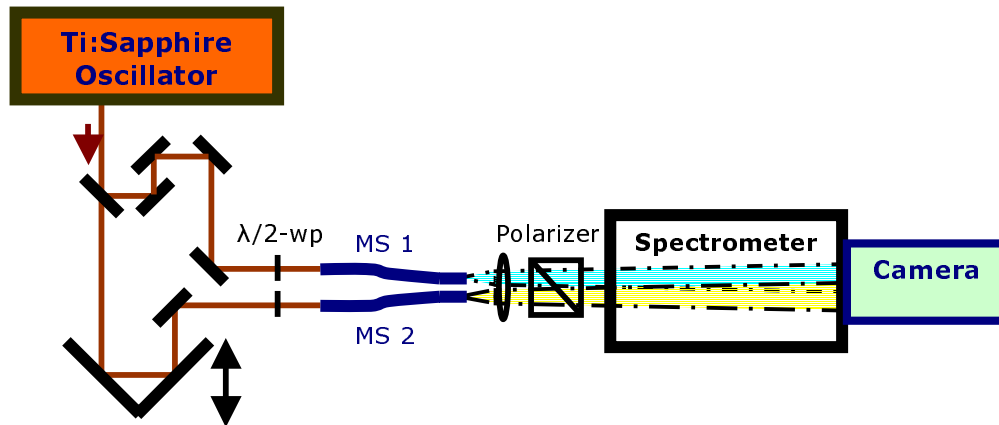


Fig. 2. Schematic diagram of the Young's double-slit-type setup. In the diagram: $\lambda/2$ -wp, half-waveplates; MS 1 and MS 2, microstructure fiber segments.

To study the SC coherence more quantitatively, the Bellini-Hänsch technique was implemented using the setup in Fig. 2. The Ti:Sapphire output was split into two pulse trains which were injected along parallel polarization eigen-axes of two separate 18-cm fiber segments to yield independently generated SC with similar characteristics. The fiber output ends were secured next to each other in the same mounting slot of a fiber chuck. The SC were then collimated by a microscope objective and passed through a linear polarizer. (Although the SC was $> 80\%$ linearly polarized, the use of a polarizer facilitates optimal comparison with the scalar simulations described below.) The objective was adjusted so that the beams expanded and overlapped at the entrance slit of a spectrometer. A slice of the overlapped beams entered the spectrometer, and the spectra at all points along the slit were recorded by a two-dimensional camera at the spectrometer exit plane, which averaged for 20 ms (1.8×10^6 pulses). The two beams were aligned so that the interference fringes were across the direction of the slit, parallel to the direction of spectral dispersion, and readily observable on the camera. The relative delay was minimized. Because of the large SC bandwidth, it was necessary to record separate interferograms over wavelength ranges 350 – 850 nm and 800 – 1500 nm, and these results are presented separately in Figs. 3(a) and (b). Well-defined interference fringes are clearly seen in the overlapped region of the two beams, indicating coherence over a wide range of wavelengths. The wavelength-dependent fringe visibility

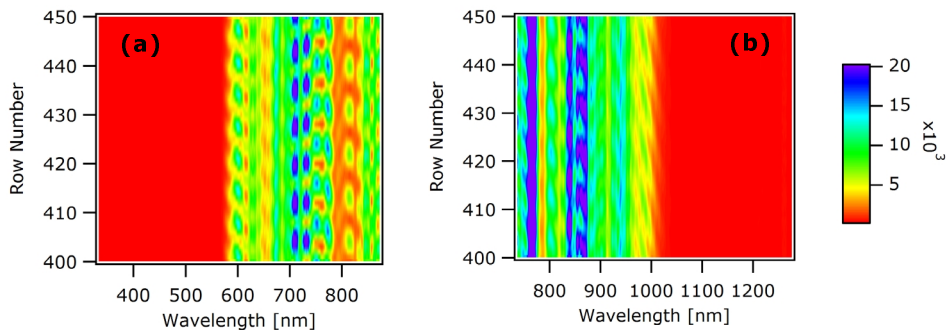


Fig. 3. Measured spatially resolved interferograms for (a) shorter- and (b) longer-wavelength sections of the SC.

$V(\lambda)$ can be easily extracted from the interferograms and, together with the measured individual SC spectra $I_1(\lambda)$ and $I_2(\lambda)$, one can calculate the magnitude of the degree of first order mutual coherence as a function of wavelength using: $|g_{12}^{(1)}(\lambda)| = \frac{V(\lambda)[I_1(\lambda) + I_2(\lambda)]}{2[I_1(\lambda)I_2(\lambda)]^{1/2}}$.

Note that the calculation of $|g_{12}^{(1)}(\lambda)|$ naturally includes differences in the interfering SC intensities, relaxing the (in-practice difficult) experimental constraint of equal injected pulse energies. Here, and elsewhere in this paper, all coherence and visibility measurements are calculated at zero relative delay between the two fields. Also note that, although the visibility was measured over 570 – 1020 nm, calculations of the coherence were restricted to the range 630 – 910 nm where the individual SC intensities were sufficiently above the measurement noise floor that nonphysical artifacts could be avoided.

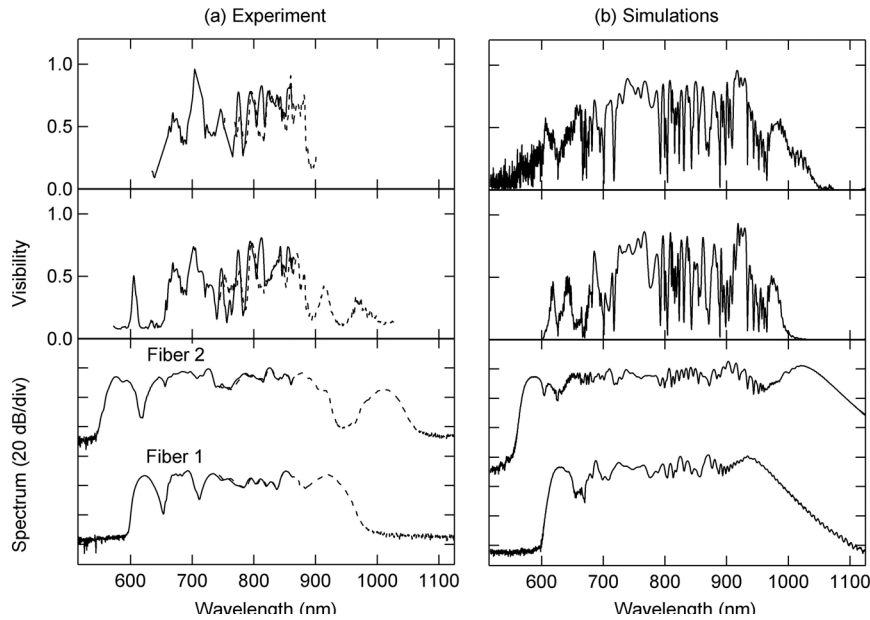


Fig. 4. (a) Experimentally measured SC spectra from each fiber (bottom), the visibility extracted from the interferogram between the two SC (middle) and the corresponding calculated degree of coherence (top). (b) corresponding results from simulations. The visibility drops near the edge of the SC spectra, due to the poor signal-to-noise ratio. The injected pulse energies are 0.25 nJ and 0.58 nJ, for the two SC pulses respectively.

Figure 4(a) shows the results of this analysis. Here, the top two panels show the visibility and the corresponding calculated degree of coherence, and the bottom panel shows the independently measured SC spectra. The solid and dashed lines correspond to measurements over the shorter and longer wavelength ranges of the SC as shown in Figs. 3(a) and (b) respectively. The visibility and degree of coherence are both high (~ 0.8) in the vicinity of the pump wavelength, confirming the spectral interference experiments described above. Away from the pump wavelength, however, a complicated wavelength dependent structure is present in both curves, and both the visibility and the coherence clearly decrease. We have found it useful to quantify these results in terms of the median visibility and degree of coherence, which we calculate to be 0.30 and 0.56 respectively. Significantly, the fact that the median degree of coherence is higher than the median visibility suggests that it is not only the loss of phase coherence which contributes to the loss of visibility, but also the fact that we were

unable to generate identical SC spectra in our experiments (which was expected, in view of the spectrum's extreme dependence on the various system parameters), so that there are differences in the interfering intensities at each wavelength. From a practical viewpoint, the median degree of coherence can be interpreted physically as providing a measure of the suitability of the SC generated under different conditions for metrology or stabilization purposes.

To interpret the experiments further, we used a stochastic NLSE model which rigorously includes input pulse and Raman noise during propagation [15]:

$$\frac{\partial E(z,t)}{\partial z} = i \sum_{k \geq 2} \frac{i^k \beta_k}{k!} \frac{\partial^k E}{\partial t^k} + i \gamma \left(1 + \frac{i}{\omega_0} \frac{\partial}{\partial t} \right) \left[E(z,t) \left(\int_{-\infty}^t R(t') |E(z,t-t')|^2 dt' + i \Gamma_R(z,t) \right) \right]$$

Here $E(z,t)$ is the pulse envelope in a co-moving frame, the β_k 's describe the fiber dispersion over 300–2000 nm, and the nonlinear coefficient $\gamma = 85 \text{ W}^{-1} \text{ km}^{-1}$ at 800 nm. The function $R(t) = (1 - f_R) \delta(t) + f_R h_R(t)$ includes instantaneous and delayed Raman contributions with the fractional Raman contribution $f_R = 0.18$. For h_R , we used the measured Raman response of silica. Spontaneous Raman noise appears as the stochastic variable Γ_R which has frequency domain correlations given by:

$\langle \Gamma_R(\Omega, z) \Gamma_R^*(\Omega, z) \rangle = (2f_R \hbar \omega_0 / \gamma) |\text{Im} h_R(\Omega)| [n_{\text{th}}(|\Omega|) + U(-\Omega)] \delta(z - z') \delta(\Omega - \Omega')$ where the thermal Bose distribution $n_{\text{th}}(\Omega) = [\exp(\hbar \Omega / k_B T) - 1]^{-1}$ and U is the Heaviside step function. The initial conditions are those of the measured pulse duration and chirp, with the addition of quantum-limited shot noise and technical noise as described below. The input pulse duration was 60 fs, and the injected pulse energies were 0.25 nJ for fiber 1 and 0.58 nJ for fiber 2, corresponding to experiments. The simulations were used to generate an ensemble of independent SC pairs $[E_1(\lambda), E_2(\lambda)]$ with different random noise seeds. From this, it is

possible to calculate both the first-order coherence $|g_{12}^{(1)}(\lambda)| = \frac{\langle E_1^*(\lambda) E_2(\lambda) \rangle}{[\langle |E_1(\lambda)|^2 \rangle \langle |E_2(\lambda)|^2 \rangle]^{1/2}}$ as

well as the corresponding fringe visibility (taking into account the different mean intensities).

Assuming shot-noise-limited input pulses in each fiber, no significant coherence degradation was observed in the simulations, with $|g_{12}^{(1)}(\lambda)| \sim 1$ at all wavelengths. This is consistent with earlier simulations [3, 4], and suggests that the observed coherence degradation in our experiments arises from other noise sources. The level of this additional noise was estimated from simulations using a simple numerical noise model based on injected peak power fluctuations, and adjusting the noise magnitude so that coherence degradation comparable to that in experiments was observed. Figure 4(b) shows simulation results assuming an input pulse noise level of 2%. Firstly, we note that the simulated mean spectra are in qualitative agreement with experiment, reproducing well the overall spectral width and the major spectral peaks at both extremes of the SC. Secondly, we see that the addition of this additional noise leads to significant coherence degradation, with median visibility and coherence of 0.35 and 0.64 respectively (calculated over the same wavelength ranges as in experiment). These results are in good agreement with experiment. Although no detailed studies were carried out to study the physical origin of this noise in more detail, additional experiments measured the level of technical injection noise at typically 0.4%. This suggests that other noise effects, possibly due to polarization instabilities also play an important role in the coherence degradation. A quantitative study of these effects, however, will require the development of a fully vectorial stochastic NLSE.

In conclusion, we have shown that the Bellini-Hansch technique has successfully allowed the first quantitative measurement of the wavelength-dependent spectral phase coherence of SC generated in microstructure fiber. Although shot-noise-limited 60-fs input pulses would be expected to yield a high degree of coherence across the entire SC spectrum, we experimentally observe significantly higher coherence degradation which exhibits strong wavelength dependence. Additional simulations allow us to estimate the magnitude of the additional noise present in the experiments as being consistent with 2% intensity fluctuations. Subsequently, we have been able to show that injection instabilities alone do not account for this level of fluctuation, suggesting that the decoherence effects most likely arise from a propagation-related instability. Since our numerical model is based on a scalar nonlinear Schrödinger equation, this suggests polarization-related effects as the most likely source of instability. Further investigations of such noise sources and their influence on the coherence will require a systematic study using the same Bellini-Hansch method employed in this paper, under a variety of conditions, including different fiber lengths, pump power levels, fiber orientations and input polarizations. Nevertheless, the stochastic NLSE simulations have reproduced well the measured mutual degree of coherence assuming 2% fluctuations in the injected peak power, and these results suggest that the generation of coherent SC will require particular care in the stabilization of the pump laser and the mechanical fiber injection conditions. With the assumption of stabilized shot-noise-limited input pulses, additional numerical studies suggest that highly coherent SC (median degree of coherence > 0.95) can be readily obtained using pulses of duration 50 fs or less, and indeed we note that this is the pulse duration range which has been used successfully for stabilization purposes [6, 8].